Position and Attitude Tracking of AUVs: A Quaternion Feedback Approach

Ola-Erik Fjellstad and Thor I. Fossen

The Norwegian Institute of Technology
Department of Engineering Cybernetics
N-7034 Trondheim, NORWAY

Abstract: A position and attitude tracking control law for autonomous underwater vehicles (AUVs) in 6 degrees of freedom (DOF) is derived. The 4-parameter unit quaternion (Euler parameters) is used in a singularity-free representation of attitude. Global convergence of the closed-loop system is proven. In addition several 3-parameter representations in terms of the Euler parameters are discussed with application to the same control law. These schemes contain singularities and only local convergence can therefore be proven. The proposed control scheme is simulated with Euler parameters and Euler angles.

1 Introduction

For rigid-bodies in 6 DOF the nonlinear dynamic equations of motion have a systematic structure which becomes apparent when applying vector notation. This is exploited in the control literature, particularly in the control of robot manipulators. A convergent nonlinear adaptive tracking control law exploiting the passivity properties of robot manipulators was derived in [19]. Later, application of this control law to 3 DOF spacecraft attitude control were made [7, 18]. This control scheme has also been extended in terms of the 6 DOF underwater vehicle equations of motion by using an Euler angle attitude representation [9].

For mobile systems in 6 DOF the dynamic equations of motion are usually separated into the translational and rotational motions. Position is specified by a three vector whereas various representations of attitude have been discussed in the literature. The most frequently applied representations are the Euler angle conventions, which all are minimal 3-parameter representations. The roll, pitch and yaw (RPY) convention dominates in the context of mobile vehicles. The popularity of the RPY-convention can probably be explained by their easily understood physical interpretation, and the fact that the Euler angles can be measured

directly with a gimbled system of gyros.一个灵巧的陀螺仪系统

Two obvious disadvantages of the Euler angle attitude representations are: (1) they are 3-parameter representations and therefore they must contain singular points [20] and (2) applying Euler angles to parameterize rotation matrices $\boldsymbol{R} \in SO(3)$, that is *Special Orthogonal* group of order 3, implies numerous computations with trigonometric functions. 1奇点2大量的三角函数计算

For conventional AUVs, the attitude is primarly horizontal with some variation due to diving. However, limited attitude control has been identified as one deficiency in the ability to properly address the work site for underwater robotic systems [24]. We believe that the free-body rotation ability is desirable for future underwater applications. More recently, strap-down navigation systems have become popular because of reduced system size, weight, power consumption and cost compared to gimbled systems of gyros. Considering strap-down navigation systems, it cannot be claimed that Euler angles are better suited than other attitude representations in control applications.

Euler parameters, or unit quaternions, have been used in different contexts of attitude control. Control of spacecraft, satellites, aircraft and helicopter are well known applications. More recently the use of Euler parameters has been reported in the robot literature. Attitude set-point regulation has been discussed in [15, 16, 17, 23], whereas others have addressed the more general problem of tracking [2, 3, 5, 18, 21]. However, the translational motion has not been addressed in these papers. Euler parameter-based set-point regulation of an underwater vehicle in 6 DOF was discussed in [6]. For the 6 DOF underwater vehicle control problems there are significant couplings between the rotational and translational motion. For instance, hydrodynamic added mass will introduce additional couplings due to added inertia, and Coriolis and centrifugal forces and moments. In addition to this, hydrodynamic damping may be strongly coupled.

In this paper the 6 DOF AUV model is written in terms of the Euler parameters to represent attitude, Section 2. In Section 3, a tracking controller is derived by applying the results in [19]. In fact, this control scheme can be viewed as an extension of the results presented in [9]. Applications to some 3-parameter attitude representations in terms of the Euler parameters is also included in Section 3. In Section 4 we present some simulation results.

2 Mathematical Modelling

2.1 Kinematic Equations of Motion

The kinematic model describes the geometrical relationship between the earth-fixed and the vehicle-fixed motions. The transformation matrix $\boldsymbol{J}(\boldsymbol{q})$ relates the body-fixed reference frame (B-frame) to the inertial reference frame (I-frame) according to:

$$\dot{\boldsymbol{\xi}} = \boldsymbol{J}(\boldsymbol{q})\boldsymbol{\nu} \;\Leftrightarrow\; \begin{bmatrix} \dot{\boldsymbol{x}} \\ \dot{\boldsymbol{q}} \end{bmatrix} = \begin{bmatrix} \boldsymbol{R}(\boldsymbol{q}) & \boldsymbol{0}_{3\times 3} \\ \boldsymbol{0}_{4\times 3} & \frac{1}{2}\boldsymbol{U}(\boldsymbol{q}) \end{bmatrix} \begin{bmatrix} \boldsymbol{v} \\ \boldsymbol{\omega} \end{bmatrix} \qquad \in \mathbb{R}^7 \tag{1}$$

where $\boldsymbol{x} = [x,\, y,\, z]^{\mathrm{T}}$ is the I-frame position of the vehicle, $\boldsymbol{q} = [\eta,\, \boldsymbol{\epsilon}^{\mathrm{T}}]^{\mathrm{T}} = [\eta,\, \epsilon_1,\, \epsilon_2,\, \epsilon_3]^{\mathrm{T}}$ is the unit quaternion representing the attitude, and $\boldsymbol{v} = [u,\, v,\, w]^{\mathrm{T}}$ and $\boldsymbol{\omega} = [p,\, q,\, r]^{\mathrm{T}}$ are the linear and angular velocities of the vehicle in the B-frame, see e.g. [11]. The elements of the unit quaternion $\boldsymbol{q} \in \mathbb{H}$ (in honour of Hamilton), are called Euler parameters and they satisfy:

$$\eta^2 + \boldsymbol{\epsilon}^{\mathrm{T}}\boldsymbol{\epsilon} = \eta^2 + \epsilon_1^2 + \epsilon_2^2 + \epsilon_3^2 = 1 \tag{2}$$

The rotation matrix $\boldsymbol{R} \in SO(3)$ from I to B in terms of the Euler parameters is written as:

$$\boldsymbol{R}(\boldsymbol{q}) = \boldsymbol{I}_{3\times 3} + 2\eta\boldsymbol{S}(\boldsymbol{\epsilon}) + 2\boldsymbol{S}^2(\boldsymbol{\epsilon}) = \begin{bmatrix} \eta^2+\epsilon_1^2-\epsilon_2^2-\epsilon_3^2 & 2(\epsilon_1\epsilon_2-\eta\epsilon_3) & 2(\epsilon_1\epsilon_3+\eta\epsilon_2) \\ 2(\epsilon_1\epsilon_2+\eta\epsilon_3) & \eta^2-\epsilon_1^2+\epsilon_2^2-\epsilon_3^2 & 2(\epsilon_2\epsilon_3-\eta\epsilon_1) \\ 2(\epsilon_1\epsilon_3-\eta\epsilon_2) & 2(\epsilon_2\epsilon_3+\eta\epsilon_1) & \eta^2-\epsilon_1^2-\epsilon_2^2+\epsilon_3^2 \end{bmatrix} \tag{3}$$

where we have used the skew-symmetric matrix $\boldsymbol{S}(\boldsymbol{a}) = -\boldsymbol{S}^{\mathrm{T}}(\boldsymbol{a})$ defined as ($\boldsymbol{a} \in \mathbb{R}^3$):

$$\boldsymbol{S}(\boldsymbol{a}) \triangleq \begin{bmatrix} 0 & -a_3 & +a_2 \\ +a_3 & 0 & -a_1 \\ -a_2 & +a_1 & 0 \end{bmatrix} \in SS(3) \tag{4}$$

such that for an arbitrary vector $\boldsymbol{b} \in \mathbb{R}^3$ we have $\boldsymbol{a} \times \boldsymbol{b} \equiv \boldsymbol{S}(\boldsymbol{a})\boldsymbol{b}$. $SS(3)$ is the set of skew-symmetric matrices of order 3. The quaternion $\boldsymbol{q}$ can be interpreted as a complex number with η being the real part and $\boldsymbol{\epsilon}$ the complex part. Hence, the complex conjugate of $\boldsymbol{q}$ is defined as:

$$\overline{\boldsymbol{q}} \triangleq \begin{bmatrix} \eta \\ -\boldsymbol{\epsilon} \end{bmatrix} \qquad \in \mathbb{H} \tag{5}$$

Accordingly, the inverse rotation matrix can be written (3):

$$\boldsymbol{R}^{-1}(\boldsymbol{q}) = \boldsymbol{R}^{\mathrm{T}}(\boldsymbol{q}) = \boldsymbol{R}(\overline{\boldsymbol{q}}) \qquad \in SO(3) \tag{6}$$

Successive rotations involves multiplication between two rotation matrices. It can be shown that:

$$\boldsymbol{R}(\boldsymbol{q}_1)\boldsymbol{R}(\boldsymbol{q}_2) = \boldsymbol{R}(\boldsymbol{q}_1\boldsymbol{q}_2) \qquad \in SO(3) \tag{7}$$

where quaternion multiplication is defined as:

$$\boldsymbol{q}_1\boldsymbol{q}_2 \triangleq \begin{bmatrix} \eta_1 & -\boldsymbol{\epsilon}_1^{\mathrm{T}} \\ \boldsymbol{\epsilon}_1 & \eta_1\boldsymbol{I}_{3\times 3} + \boldsymbol{S}(\boldsymbol{\epsilon}_1) \end{bmatrix} \begin{bmatrix} \eta_2 \\ \boldsymbol{\epsilon}_2 \end{bmatrix} \qquad \in \mathbb{H} \tag{8}$$

The set of unit quaternions $\mathbb{H}$ together with quaternion multiplication forms a group of infinite order. The coordinate transformation matrix $\boldsymbol{U}(\boldsymbol{q})$ can be written as:

$$\boldsymbol{U}(\boldsymbol{q}) = \begin{bmatrix} -\boldsymbol{\epsilon}^{\mathrm{T}} \\ \eta\boldsymbol{I}_{3\times 3} + \boldsymbol{S}(\boldsymbol{\epsilon}) \end{bmatrix} = \begin{bmatrix} -\boldsymbol{\epsilon}^{\mathrm{T}} \\ \boldsymbol{T}(\boldsymbol{q}) \end{bmatrix} \qquad \in \mathbb{R}^{4\times 3} \tag{9}$$

The 7×6 transformation matrix $\boldsymbol{J}(\boldsymbol{q})$ has full rank: $\mathrm{rank}[\boldsymbol{J}(\boldsymbol{q})] = 6\,\forall\,\boldsymbol{q} \in \mathbb{H}$. Hence the kinematic equations contain no singular points. The computation of the kinematic equations

involves multiplications and additions only. No function evaluations are needed. Moreover, the rotational kinematic equations are linear in $\boldsymbol{q}$ (and $\boldsymbol{\omega}$).

2.2 Rigid-Body Dynamics

Newton's equations of motion for a rigid-body with constant mass are written [10]:

$$m[\dot{\boldsymbol{v}} + \boldsymbol{\omega} \times \boldsymbol{v} + \dot{\boldsymbol{\omega}} \times \boldsymbol{r}_G + \boldsymbol{\omega} \times (\boldsymbol{\omega} \times \boldsymbol{r}_G)] = \boldsymbol{f}_1 \tag{10}$$

$$\boldsymbol{I}_0\, \dot{\boldsymbol{\omega}} + \boldsymbol{\omega} \times (\boldsymbol{I}_0\, \boldsymbol{\omega}) + m\boldsymbol{r}_G \times (\dot{\boldsymbol{v}} + \boldsymbol{\omega} \times \boldsymbol{v}) = \boldsymbol{f}_2 \tag{11}$$

where $\boldsymbol{r}_G = [x_G,\, y_G,\, z_G]^{\mathrm{T}}$ is the center of gravity, m is the constant mass, $\boldsymbol{I}_0 = \boldsymbol{I}_0^{\mathrm{T}} > \boldsymbol{0}_{3\times 3}$ is the inertia matrix of the vehicle with respect to the B-frame origin, and $\boldsymbol{f}_1$ and $\boldsymbol{f}_2$ are vectors of external applied forces and moments, respectively. To exploit the structure of the dynamic equations in the control design, we write (10) and (11) in a more compact form as [8]:

$$\boldsymbol{M}_{RB}\dot{\boldsymbol{\nu}} + \boldsymbol{C}_{RB}(\boldsymbol{\nu})\boldsymbol{\nu} = \boldsymbol{\tau}_{RB} \tag{12}$$

where $\boldsymbol{\tau}_{RB} = [\boldsymbol{f}_1^{\mathrm{T}},\, \boldsymbol{f}_2^{\mathrm{T}}]^{\mathrm{T}}$ and

$$\boldsymbol{M}_{RB} = \begin{bmatrix} m\boldsymbol{I}_{3\times 3} & -m\boldsymbol{S}(\boldsymbol{r}_G) \\ m\boldsymbol{S}(\boldsymbol{r}_G) & \boldsymbol{I}_0 \end{bmatrix} \tag{13}$$

$$\boldsymbol{C}_{RB}(\boldsymbol{\nu}) = \begin{bmatrix} \boldsymbol{0}_{3\times 3} & -m\boldsymbol{S}(\boldsymbol{v}) - m\boldsymbol{S}(\boldsymbol{S}(\boldsymbol{\omega})\boldsymbol{r}_G) \\ -m\boldsymbol{S}(\boldsymbol{v}) - m\boldsymbol{S}(\boldsymbol{S}(\boldsymbol{\omega})\boldsymbol{r}_G) & -\boldsymbol{S}(\boldsymbol{I}_0\boldsymbol{\omega}) + m\boldsymbol{S}(\boldsymbol{S}(\boldsymbol{v})\boldsymbol{r}_G) \end{bmatrix} \tag{14}$$

Notice that the term $\mathrm{m}\boldsymbol{S}(\boldsymbol{v})\boldsymbol{v} = \boldsymbol{0}$ is added to make $\boldsymbol{C}_{RB}(\boldsymbol{\nu})$ skew-symmetrical. This term is only used in the convergence proof and is not necessary when implementing the control law.

2.3 Added Inertia

According to [12] the added mass derivatives for a completely submerged vehicle in an ideal fluid are functions of body shape and the density of the fluid. Moreover, wave frequency independence can be assumed under the assumption that the vehicle is operating below the wave affected zone (depth $\gg$ 20 m). Variations of water density is considered negligible for control applications. The numerical values of added mass in a real fluid are usually in good agreement with those obtained from ideal fluid theory [22]. Hence, the added inertia matrix

$\boldsymbol{M}_A$ is assumed to be positive definite and constant:

$$\boldsymbol{M}_A = -\left[\begin{array}{ccc|ccc} X_{\dot{u}} & X_{\dot{v}} & X_{\dot{w}} & X_{\dot{p}} & X_{\dot{q}} & X_{\dot{r}} \\ Y_{\dot{u}} & Y_{\dot{v}} & Y_{\dot{w}} & Y_{\dot{p}} & Y_{\dot{q}} & Y_{\dot{r}} \\ Z_{\dot{u}} & Z_{\dot{v}} & Z_{\dot{w}} & Z_{\dot{p}} & Z_{\dot{q}} & Z_{\dot{r}} \\ \hline K_{\dot{u}} & K_{\dot{v}} & K_{\dot{w}} & K_{\dot{p}} & K_{\dot{q}} & K_{\dot{r}} \\ M_{\dot{u}} & M_{\dot{v}} & M_{\dot{w}} & M_{\dot{p}} & M_{\dot{q}} & M_{\dot{r}} \\ N_{\dot{u}} & N_{\dot{v}} & N_{\dot{w}} & N_{\dot{p}} & N_{\dot{q}} & N_{\dot{r}} \end{array}\right] = \left[\begin{array}{cc} \boldsymbol{A}_{11} & \boldsymbol{A}_{12} \\ \boldsymbol{A}_{21} & \boldsymbol{A}_{22} \end{array}\right] \tag{15}$$

where $\boldsymbol{A}_{11} = \boldsymbol{A}_{11}^{\mathrm{T}}$, $\boldsymbol{A}_{12} = \boldsymbol{A}_{21}^{\mathrm{T}}$, and $\boldsymbol{A}_{22} = \boldsymbol{A}_{22}^{\mathrm{T}}$. The concept of added mass introduces Coriolis and centrifugal terms. These extra terms can be represented by $\boldsymbol{C}_A(\boldsymbol{\nu})\boldsymbol{\nu}$ where; see (13) and (14):

$$\boldsymbol{C}_A(\boldsymbol{\nu}) = \left[\begin{array}{cc} \boldsymbol{0}_{3\times 3} & -\boldsymbol{S}(\boldsymbol{A}_{11}\boldsymbol{v} + \boldsymbol{A}_{12}\boldsymbol{\omega}) \\ -\boldsymbol{S}(\boldsymbol{A}_{11}\boldsymbol{v} + \boldsymbol{A}_{12}\boldsymbol{\omega}) & -\boldsymbol{S}(\boldsymbol{A}_{21}\boldsymbol{v} + \boldsymbol{A}_{22}\boldsymbol{\omega}) \end{array}\right] \tag{16}$$

This matrix is skew-symmetrical. The derivation of $\boldsymbol{C}_A(\boldsymbol{\nu})$ is based on Kirchoff's equations [14].

2.4 Hydrodynamic Damping

The dissipative forces and moments due to hydrodynamic damping are collected in the vector term $\boldsymbol{D}(\boldsymbol{\nu})\boldsymbol{\nu}$. This term should at least include quadratic drag and lift. In addition, laminar and turbulent skin friction due to boundary layer flow, and viscous damping due to vortex shedding can be modelled [4]. The wave-induced forces and moments ware assumed to be negligible for vehicles operating below the wave affected zone (depth $\gg$ 20m). The matrix $\boldsymbol{D}(\boldsymbol{\nu})$ will be strictly positive, that is:

$$\boldsymbol{D}(\boldsymbol{\nu}) > \boldsymbol{0}_{6\times 6} \tag{17}$$

such that $\boldsymbol{\nu}^{\mathrm{T}}\boldsymbol{D}(\boldsymbol{\nu})\boldsymbol{\nu} > 0\,\forall\,\boldsymbol{\nu} \neq \boldsymbol{0}$. This reflects the dissipative nature of the hydrodynamic forces and moments.

2.5 Restoring Forces and Moments

The gravitational and buoyant forces are written $W = mg$ and $B = \rho g \nabla$ where ρ is the mass density of water and ∇ is the volume of the displaced water. They act through the center of gravity $\boldsymbol{r}_G = [x_G,\, y_G,\, z_G]^{\mathrm{T}}$ and the center of buoyancy $\boldsymbol{r}_B = [x_B,\, y_B,\, z_B]^{\mathrm{T}}$, respectively. Transforming the weight and the buoyancy to the B-frame yields:

$$\boldsymbol{f}_G = \boldsymbol{R}^{\mathrm{T}}(\boldsymbol{q})\left[\begin{array}{c} 0 \\ 0 \\ W \end{array}\right], \qquad \boldsymbol{f}_B = \boldsymbol{R}^{\mathrm{T}}(\boldsymbol{q})\left[\begin{array}{c} 0 \\ 0 \\ B \end{array}\right] \tag{18}$$

Notice that the I-frame z-axis is taken to be positive downwards. The restoring forces and moments are collected in a vector $\boldsymbol{g}(\boldsymbol{q})$ according to:

$$\boldsymbol{g}(\boldsymbol{q}) = \begin{bmatrix} \boldsymbol{f}_B - \boldsymbol{f}_G \\ \boldsymbol{r}_B \times \boldsymbol{f}_B - \boldsymbol{r}_G \times \boldsymbol{f}_G \end{bmatrix} \tag{19}$$

which can be written in component form:

$$\boldsymbol{g}(\boldsymbol{q}) = \begin{bmatrix} 2\,(\eta\epsilon_2 - \epsilon_1\,\epsilon_3)\,(W - B) \\ -2\,(\eta\epsilon_1 + \epsilon_2\,\epsilon_3)\,(W - B) \\ (-\eta^2 + \epsilon_1^2 + \epsilon_2^2 - \epsilon_3^2)\,(W - B) \\ (-\eta^2 + \epsilon_1^2 + \epsilon_2^2 - \epsilon_3^2)\,(y_G\,W - y_B\,B) + 2\,(\eta\epsilon_1 + \epsilon_2\,\epsilon_3)\,(z_G\,W - z_B\,B) \\ -\,(-\eta^2 + \epsilon_1^2 + \epsilon_2^2 - \epsilon_3^2)\,(x_G\,W - x_B\,B) + 2\,(\eta\epsilon_2 - \epsilon_1\,\epsilon_3)\,(z_G\,W - z_B\,B) \\ -2\,(\eta\epsilon_1 + \epsilon_2\,\epsilon_3)\,(x_G\,W - x_B\,B) - 2\,(\eta\epsilon_2 - \epsilon_1\,\epsilon_3)\,(y_G\,W - y_B\,B) \end{bmatrix} \tag{20}$$

2.6 Dynamic Equations of Motion in the B-Frame

The rigid-body dynamics and the added inertia, hydrodynamic damping and restoring forces and moments yields the total dynamic model in the B-frame:

$$\boldsymbol{M}\dot{\boldsymbol{\nu}} + \boldsymbol{C}(\boldsymbol{\nu})\boldsymbol{\nu} + \boldsymbol{D}(\boldsymbol{\nu})\boldsymbol{\nu} + \boldsymbol{g}(\boldsymbol{q}) = \boldsymbol{\tau} \tag{21}$$

where

$$\boldsymbol{M} = \boldsymbol{M}_{RB} + \boldsymbol{M}_A = \begin{bmatrix} \boldsymbol{M}_{11} & \boldsymbol{M}_{12} \\ \boldsymbol{M}_{21} & \boldsymbol{M}_{22} \end{bmatrix}, \tag{22}$$

$$\boldsymbol{C}(\boldsymbol{\nu}) = \boldsymbol{C}_{RB}(\boldsymbol{\nu}) + \boldsymbol{C}_A(\boldsymbol{\nu}) = \begin{bmatrix} \boldsymbol{0}_{3\times3} & -\boldsymbol{S}(\boldsymbol{M}_{11}\boldsymbol{v} + \boldsymbol{M}_{12}\boldsymbol{\omega}) \\ -\boldsymbol{S}(\boldsymbol{M}_{11}\boldsymbol{v} + \boldsymbol{M}_{12}\boldsymbol{\omega}) & -\boldsymbol{S}(\boldsymbol{M}_{21}\boldsymbol{v} + \boldsymbol{M}_{22}\boldsymbol{\omega}) \end{bmatrix} \tag{23}$$

and $\boldsymbol{\tau}$ is a vector of actuator control forces and moments. Notice that $\boldsymbol{M}$ is assumed to be constant and positive definite, and $\boldsymbol{C}(\boldsymbol{\nu})$ is skew-symmetrical; that is:

$$\boldsymbol{M} = \boldsymbol{M}^{\mathrm{T}} > \boldsymbol{0}_{6\times6}, \qquad \dot{\boldsymbol{M}} = \boldsymbol{0}_{6\times6} \tag{24}$$

$$\boldsymbol{C}(\boldsymbol{\nu}) = -\boldsymbol{C}^{\mathrm{T}}(\boldsymbol{\nu}) \qquad \in SS(6) \tag{25}$$

2.7 Dynamic Equations of Motion in the I-Frame

The dynamic equations of motion (21) can be formulated in the I-frame by utilizing the following relationships (arguments are omitted to increase readability):

$$\boldsymbol{J}^+ = (\boldsymbol{J}^{\mathrm{T}}\boldsymbol{J})^{-1}\boldsymbol{J}^{\mathrm{T}} = \begin{bmatrix} \boldsymbol{R}^{\mathrm{T}} & \boldsymbol{0}_{3\times4} \\ \boldsymbol{0}_{3\times3} & 2\boldsymbol{U}^{\mathrm{T}} \end{bmatrix} \;\Rightarrow\; \boldsymbol{J}^+\boldsymbol{J} = \boldsymbol{I}_{6\times6} \tag{26}$$

$$\dot{\boldsymbol{\xi}} = \boldsymbol{J}\boldsymbol{\nu} \;\Rightarrow\; \boldsymbol{\nu} = \boldsymbol{J}^+\dot{\boldsymbol{\xi}} \;\Rightarrow\; \dot{\boldsymbol{\nu}} = \dot{\boldsymbol{J}}^+\dot{\boldsymbol{\xi}} + \boldsymbol{J}^+\ddot{\boldsymbol{\xi}} \tag{27}$$

Here, the 6×7 matrix $\boldsymbol{J}^+$ is the generalized left inverse of $\boldsymbol{J}$ and the time derivative is denoted $\mathrm{d}/\mathrm{d}t[\boldsymbol{J}^+] = \dot{\boldsymbol{J}}^+$. Substituting (26) and (27) into (21) yields:

$$\boldsymbol{M}^*\ddot{\boldsymbol{\xi}} + \boldsymbol{C}^*\dot{\boldsymbol{\xi}} + \boldsymbol{D}^*\dot{\boldsymbol{\xi}} + \boldsymbol{g}^* = \boldsymbol{\tau}^* \tag{28}$$

where

$$\begin{aligned}
\boldsymbol{M}^*(\boldsymbol{q}) &= \boldsymbol{J}^{+\mathrm{T}}(\boldsymbol{q})\boldsymbol{M}\boldsymbol{J}^+(\boldsymbol{q}) && (29)\\
\boldsymbol{C}^*(\boldsymbol{q},\dot{\boldsymbol{\xi}}) &= \boldsymbol{J}^{+\mathrm{T}}(\boldsymbol{q})\boldsymbol{C}(\boldsymbol{\nu})\boldsymbol{J}^+(\boldsymbol{q}) + \boldsymbol{J}^{+\mathrm{T}}(\boldsymbol{q})\boldsymbol{M}\dot{\boldsymbol{J}}^+(\boldsymbol{q},\dot{\boldsymbol{q}}) && (30)\\
\boldsymbol{D}^*(\boldsymbol{q},\dot{\boldsymbol{\xi}}) &= \boldsymbol{J}^{+\mathrm{T}}(\boldsymbol{q})\boldsymbol{D}(\boldsymbol{\nu})\boldsymbol{J}^+(\boldsymbol{q}) && (31)\\
\boldsymbol{g}^*(\boldsymbol{q}) &= \boldsymbol{J}^{+\mathrm{T}}(\boldsymbol{q})\boldsymbol{g} && (32)\\
\boldsymbol{\tau}^*(\boldsymbol{q}) &= \boldsymbol{J}^{+\mathrm{T}}(\boldsymbol{q})\boldsymbol{\tau} && (33)
\end{aligned}$$

From (17), (24) and (25) it can be shown that $\boldsymbol{M}^*(\boldsymbol{q})$ is positive semidefinite, $\boldsymbol{D}^*(\boldsymbol{q},\dot{\boldsymbol{\xi}})$ is positive and $\dot{\boldsymbol{M}}^*(\boldsymbol{q}) - 2\boldsymbol{C}^*(\boldsymbol{q},\dot{\boldsymbol{\xi}})$ is skew-symmetrical, that is:

$$\begin{aligned}
\boldsymbol{y}^{\mathrm{T}}\boldsymbol{M}^*(\boldsymbol{q})\boldsymbol{y} &> 0, \qquad \forall\, \boldsymbol{y} \neq \alpha \begin{bmatrix} \boldsymbol{0} \\ \boldsymbol{q} \end{bmatrix}, \qquad \alpha \in \mathbb{R} && (34)\\
\boldsymbol{y}^{\mathrm{T}}\boldsymbol{D}^*(\boldsymbol{q},\dot{\boldsymbol{\xi}})\boldsymbol{y} &> 0, \qquad \forall\, \boldsymbol{y} \neq \alpha \begin{bmatrix} \boldsymbol{0} \\ \boldsymbol{q} \end{bmatrix}, \qquad \alpha \in \mathbb{R} && (35)\\
[\dot{\boldsymbol{M}}^*(\boldsymbol{q}) - 2\boldsymbol{C}^*(\boldsymbol{q},\dot{\boldsymbol{\xi}})] &= -[\dot{\boldsymbol{M}}^*(\boldsymbol{q}) - 2\boldsymbol{C}^*(\boldsymbol{q},\dot{\boldsymbol{\xi}})]^{\mathrm{T}} && (36)
\end{aligned}$$

These properties will be exploited in the convergence analysis of the proposed control laws. Notice that $\boldsymbol{C}^*(\boldsymbol{q},\dot{\boldsymbol{\xi}})$ is not skew-symmetrical. Moreover:

$$\boldsymbol{C}^{*\mathrm{T}}(\boldsymbol{q},\dot{\boldsymbol{\xi}}) \neq -\boldsymbol{C}^*(\boldsymbol{q},\dot{\boldsymbol{\xi}}) \tag{37}$$

3 Main Results

Attitude control of underwater vehicles has traditionally been done in terms of the 3-parameter Euler angle representation. Consequently, global convergence cannot be obtained due to singularities which are introduced in all minimal representations of the 3D rotation group. We propose to use the Euler parameters (unit quaternion) for attitude representation of underwater vehicles in order to allow free-body rotations. The 6 DOF model properties derived in Section 2 are utilized in the design of a *globally* convergent tracking control law for underwater vehicles.

3.1 Unit Quaternion Feedback (4-Parameter Representation)

In this section a 6 DOF tracking controller for AUVs is presented. The proposed control law is based on the unit quaternions attitude representation of Section 2. Global convergence of the closed-loop system is guaranteed by using standard stability analysis [13].

The tracking error is chosen as the arithmetic difference between the actual and the desired position and attitude:

$$\tilde{\boldsymbol{\xi}} = \boldsymbol{\xi} - \boldsymbol{\xi}_d \tag{38}$$

where $\boldsymbol{\xi}_d$ is the desired position and attitude vector. Define a measure of tracking error $\boldsymbol{s} \in \mathbb{R}^7$ as [19]:

$$\boldsymbol{s} \triangleq \boldsymbol{K}_D \dot{\tilde{\boldsymbol{\xi}}} + \boldsymbol{K}_P \tilde{\boldsymbol{\xi}} + \boldsymbol{K}_I \int_{t_0}^{t} \tilde{\boldsymbol{\xi}}(\tau)\mathrm{d}\tau = \boldsymbol{K}_D \dot{\boldsymbol{\xi}} - \dot{\boldsymbol{\xi}}_r \tag{39}$$

$$\Rightarrow \dot{\boldsymbol{\xi}}_r \triangleq \boldsymbol{K}_D \dot{\boldsymbol{\xi}}_d - \boldsymbol{K}_P \tilde{\boldsymbol{\xi}} - \boldsymbol{K}_I \int_{t_0}^{t} \tilde{\boldsymbol{\xi}}(\tau)\mathrm{d}\tau \tag{40}$$

where $\boldsymbol{K}_D = \boldsymbol{K}_D^{\mathrm{T}} > \boldsymbol{0}_{7\times 7}$ and $\boldsymbol{K}_I = \boldsymbol{K}_I^{\mathrm{T}} > \boldsymbol{0}_{7\times 7}$ are positive definite, and $\boldsymbol{K}_P > \boldsymbol{0}_{7\times 7}$ is strictly positive. The vector $\dot{\boldsymbol{\xi}}_r$ can be interpreted as a virtual velocity reference signal. Consider the positive semi-definite function:

$$V = \frac{1}{2}\boldsymbol{s}^{\mathrm{T}}\boldsymbol{M}^*(\boldsymbol{q})\boldsymbol{s} > 0, \qquad \forall\, \boldsymbol{s} \neq \alpha \begin{bmatrix} \boldsymbol{0} \\ \boldsymbol{q} \end{bmatrix}, \qquad \alpha \in \mathbb{R} \tag{41}$$

Differentiation of (41) with respect to time yields:

$$\begin{aligned} \dot{V} &= \frac{1}{2}\boldsymbol{s}^{\mathrm{T}}\dot{\boldsymbol{M}}^*\boldsymbol{s} + \boldsymbol{s}^{\mathrm{T}}\boldsymbol{M}^*\dot{\boldsymbol{s}} \\ &= \boldsymbol{s}^{\mathrm{T}}[\boldsymbol{\tau}^* - \boldsymbol{M}^*\ddot{\boldsymbol{\xi}}_r - \boldsymbol{C}^*\dot{\boldsymbol{\xi}}_r - \boldsymbol{D}^*\dot{\boldsymbol{\xi}}_r - \boldsymbol{g}^*] - \boldsymbol{s}^{\mathrm{T}}\boldsymbol{D}^*\boldsymbol{s} \end{aligned} \tag{42}$$

where the properties (34) and (36) have been utilized. By choosing the control law as:

$$\boldsymbol{\tau}^* = \boldsymbol{M}^*\ddot{\boldsymbol{\xi}}_r + \boldsymbol{C}^*\dot{\boldsymbol{\xi}}_r + \boldsymbol{D}^*\dot{\boldsymbol{\xi}}_r + \boldsymbol{g}^* - \boldsymbol{\Lambda}\boldsymbol{s} \tag{43}$$

where $\boldsymbol{\Lambda} > \boldsymbol{0} \in \mathbb{R}^{7\times 7}$ is strictly positive, $\dot{V}$ becomes strictly negative:

$$\dot{V} = -\boldsymbol{s}^{\mathrm{T}}[\boldsymbol{\Lambda} + \boldsymbol{D}^*]\boldsymbol{s} < 0, \qquad \forall\, \boldsymbol{s} \neq \boldsymbol{0} \tag{44}$$

In this case we cannot use Lyapunov's theorems for non-autonomous systems since V is only positive semi-definite. However, if we assume that the inertial virtual velocity reference vector is two times differentiable, $\dot{\boldsymbol{\xi}}_r \in C^2[\mathbb{R}_+] \times \mathbb{R}^7$, then $\ddot{V}$ is bounded, and consequently $\dot{V}$ is uniformly continuous. Hence application of Barbălat's Lemma [1, 13] guarantees globally convergence of $\boldsymbol{s} \to \boldsymbol{0}$ as $t \to \infty$. Finally, tracking is obtained according to:

$$\boldsymbol{s} = \boldsymbol{K}_D \dot{\tilde{\boldsymbol{\xi}}} + \boldsymbol{K}_P \tilde{\boldsymbol{\xi}} + \boldsymbol{K}_I \int_{t_0}^{t} \tilde{\boldsymbol{\xi}}(\tau)\mathrm{d}\tau \;\to\; \boldsymbol{0} \;\Rightarrow\; \tilde{\boldsymbol{\xi}} \;\to\; \boldsymbol{0} \tag{45}$$

Notice that globally convergence of $\tilde{\boldsymbol{\xi}} \rightarrow \mathbf{0}$ is guaranteed also when $\boldsymbol{K}_I = \mathbf{0}$, that is the integral action can be removed in case of no unmodelled external disturbances. We define the B-frame virtual velocity reference $\boldsymbol{\nu}_r$ as:

$$\boldsymbol{\nu}_r \stackrel{\triangle}{=} \boldsymbol{J}^{+}(\boldsymbol{q})\dot{\boldsymbol{\xi}}_r \tag{46}$$

The control law (43) can then be written in the$B$-frame as:

$$\boldsymbol{\tau} = \boldsymbol{M}\dot{\boldsymbol{\nu}}_r + \boldsymbol{C}(\boldsymbol{\nu})\boldsymbol{\nu}_r + \boldsymbol{D}(\boldsymbol{\nu})\boldsymbol{\nu}_r + \boldsymbol{g}(\boldsymbol{q}) - \boldsymbol{J}^{\mathrm{T}}(\boldsymbol{q})\boldsymbol{K}_D\boldsymbol{s} \tag{47}$$

This result is similar to the locally convergent control law of [9], except that Euler parameters are used in a singularity-free representation of the attitude. Hence the control law (47) is globally convergent. An extension to adaptive control is straightforward if the dynamic model is linear in the unknown parameters which usually is the case for mechanical systems.

3.2 Application to 3-Parameter Attitude Representations

All minimal 3-parameter representations of attitude contain at least one singularity [20]. The various Euler angles representations are well known examples. In this section we discuss some alternative 3-parameter representations in terms of the Euler parameters and with application to the proposed controller.

The following kinematic models are given:

$$\text{Vector quaternion:} \qquad \dot{\boldsymbol{\xi}}_1 = \boldsymbol{J}_1(\boldsymbol{q})\boldsymbol{\nu} \Leftrightarrow \begin{bmatrix} \dot{\boldsymbol{x}} \\ \dot{\boldsymbol{\epsilon}} \end{bmatrix} = \begin{bmatrix} \boldsymbol{R}(\boldsymbol{q}) & \mathbf{0}_{3\times 3} \\ \mathbf{0}_{3\times 3} & \frac{1}{2}\boldsymbol{T}(\boldsymbol{q}) \end{bmatrix} \begin{bmatrix} \boldsymbol{v} \\ \boldsymbol{\omega} \end{bmatrix} \tag{48}$$

$$\text{Euler rotation:} \qquad \dot{\boldsymbol{\xi}}_2 = \boldsymbol{J}_2(\boldsymbol{q})\boldsymbol{\nu} \Leftrightarrow \begin{bmatrix} \dot{\boldsymbol{x}} \\ (\dot{\eta\boldsymbol{\epsilon}}) \end{bmatrix} = \begin{bmatrix} \boldsymbol{R}(\boldsymbol{q}) & \mathbf{0}_{3\times 3} \\ \mathbf{0}_{3\times 3} & \frac{1}{2}\boldsymbol{E}(\boldsymbol{q}) \end{bmatrix} \begin{bmatrix} \boldsymbol{v} \\ \boldsymbol{\omega} \end{bmatrix} \tag{49}$$

$$\text{Rodrigues parameter:} \qquad \dot{\boldsymbol{\xi}}_3 = \boldsymbol{J}_3(\boldsymbol{q})\boldsymbol{\nu} \Leftrightarrow \begin{bmatrix} \dot{\boldsymbol{x}} \\ (\dot{\boldsymbol{\epsilon}/\eta}) \end{bmatrix} = \begin{bmatrix} \boldsymbol{R}(\boldsymbol{q}) & \mathbf{0}_{3\times 3} \\ \mathbf{0}_{3\times 3} & \frac{1}{2}\boldsymbol{F}(\boldsymbol{q}) \end{bmatrix} \begin{bmatrix} \boldsymbol{v} \\ \boldsymbol{\omega} \end{bmatrix} \tag{50}$$

where the attitude transformation matrices are defined as:

$$\boldsymbol{T}(\boldsymbol{q}) = \eta\boldsymbol{I}_{3\times 3} + \boldsymbol{S}(\boldsymbol{\epsilon}) \tag{51}$$

$$\boldsymbol{E}(\boldsymbol{q}) = \eta^2\boldsymbol{I}_{3\times 3} + \eta\boldsymbol{S}(\boldsymbol{\epsilon}) - \boldsymbol{\epsilon}\boldsymbol{\epsilon}^{\mathrm{T}} \tag{52}$$

$$\boldsymbol{F}(\boldsymbol{q}) = \boldsymbol{I}_{3\times 3} + \frac{1}{\eta}\boldsymbol{S}(\boldsymbol{\epsilon}) + \frac{1}{\eta^2}\boldsymbol{\epsilon}\boldsymbol{\epsilon}^{\mathrm{T}} \tag{53}$$

The proposed unified 3-parameter feedback control law becomes:

$$\boldsymbol{\tau}_j = \boldsymbol{M}\dot{\boldsymbol{\nu}}_{rj} + \boldsymbol{C}(\boldsymbol{\nu})\boldsymbol{\nu}_{rj} + \boldsymbol{D}(\boldsymbol{\nu})\boldsymbol{\nu}_{rj} + \boldsymbol{g}(\boldsymbol{q}) - \boldsymbol{J}_j^{\mathrm{T}}(\boldsymbol{q})\boldsymbol{\Lambda}\boldsymbol{s}_j; \qquad (j = 1...3) \tag{54}$$

where

$$\boldsymbol{\nu}_{rj} \triangleq \boldsymbol{J}_j^{-1}(\boldsymbol{q})\,\dot{\boldsymbol{\xi}}_{rj}; \qquad (j = 1...3) \tag{55}$$

$$\boldsymbol{s}_j \triangleq \boldsymbol{K}_D\,\dot{\tilde{\boldsymbol{\xi}}}_j + \boldsymbol{K}_P\,\tilde{\boldsymbol{\xi}}_j + \boldsymbol{K}_I \int_{t_0}^{t} \tilde{\boldsymbol{\xi}}_j(\tau)\mathrm{d}\tau = \boldsymbol{K}_D\,\dot{\boldsymbol{\xi}}_j - \dot{\boldsymbol{\xi}}_{rj}; \quad (j = 1...3) \tag{56}$$

$$\Rightarrow \dot{\boldsymbol{\xi}}_{rj} \triangleq \boldsymbol{K}_D\,\dot{\boldsymbol{\xi}}_{dj} - \boldsymbol{K}_P\,\tilde{\boldsymbol{\xi}}_j - \boldsymbol{K}_I \int_{t_0}^{t} \tilde{\boldsymbol{\xi}}_j(\tau)\mathrm{d}\tau; \qquad (j = 1...3) \tag{57}$$

where $\boldsymbol{K}_D = \boldsymbol{K}_D^{\mathrm{T}} > \boldsymbol{0}_{6\times 6}$, and $\boldsymbol{K}_I = \boldsymbol{K}_I^{\mathrm{T}} > \boldsymbol{0}_{6\times 6}$ are positive definite, and $\boldsymbol{K}_P > \boldsymbol{0}_{6\times 6}$ and $\boldsymbol{\Lambda} > \boldsymbol{0}_{6\times 6}$ are strictly positive. If we substitute $\boldsymbol{\xi}_j$ for $\boldsymbol{\xi}$ and $\boldsymbol{J}_j$ for $\boldsymbol{J}$ in Section 2, the properties (34), (35) and (36) are still valid in all three cases ($j = 1...3$) except at the representation singularities. In case of the vector quaternion and Rodrigues parameter representations the singularity is at $\eta = 0$, while $\boldsymbol{E}(\boldsymbol{q})$ is singular for $\eta \in \{0, \pm 1/\sqrt{2}\}$. Hence, the convergence analysis in the previous section can be used to prove local convergence for all three attitude representations. The inverse Jacobians can be written ($\boldsymbol{J}_j^{-1} = \boldsymbol{J}_j^{+}$):

$$\boldsymbol{J}_1^{-1} = \begin{bmatrix} \boldsymbol{R}^{\mathrm{T}} & \boldsymbol{0} \\ \boldsymbol{0} & 2\boldsymbol{T}^{-1} \end{bmatrix}, \qquad \boldsymbol{J}_2^{-1} = \begin{bmatrix} \boldsymbol{R}^{\mathrm{T}} & \boldsymbol{0} \\ \boldsymbol{0} & 2\boldsymbol{E}^{-1} \end{bmatrix}, \qquad \boldsymbol{J}_3^{-1} = \begin{bmatrix} \boldsymbol{R}^{\mathrm{T}} & \boldsymbol{0} \\ \boldsymbol{0} & 2\boldsymbol{F}^{-1} \end{bmatrix} \tag{58}$$

where the inverse attitude transformation matrices are found as:

$$\boldsymbol{T}^{-1}(\boldsymbol{q}) = \eta\boldsymbol{I}_{3\times 3} - \boldsymbol{S}(\boldsymbol{\epsilon}) + \frac{1}{\eta}\boldsymbol{\epsilon}\boldsymbol{\epsilon}^{\mathrm{T}} \tag{59}$$

$$\boldsymbol{E}^{-1}(\boldsymbol{q}) = \boldsymbol{I}_{3\times 3} - \frac{1}{\eta}\boldsymbol{S}(\boldsymbol{\epsilon}) + \frac{2}{2\eta^2 - 1}\boldsymbol{\epsilon}\boldsymbol{\epsilon}^{\mathrm{T}} \tag{60}$$

$$\boldsymbol{F}^{-1}(\boldsymbol{q}) = \eta^2\boldsymbol{I}_{3\times 3} - \eta\boldsymbol{S}(\boldsymbol{\epsilon}) \tag{61}$$

There is a fundamental difference between these three attitude representations and the RPY Euler angles representations. For the vector quaternion and the Rodrigues parameter representations, the x_B-, y_B- and z_B-axes may point in any inertial direction except $-x_I$, $-y_I$ and $-z_I$, respectively. These configurations always gives singularities in the kinematic equations. In addition, for all other directions of the x_B-, y_B- and z_B-axes there exist one singular configuration. Moreover, choosing a direction for the x_B-axis for instance, there is one pair y_B and z_B such that the kinematic equations are singular. On the contrary, for the RPY parameters there are only two directions for the x_B-axis which causes problems, namely $x_B = \pm z_I$. The dissimilarity is explained from the definitions of the parameters. In other words the Euler angles come from composite rotations, whereas the others may be derived from a single rotation.

4 Simulation Study

The control law has been simulated for an underwater vehicle in 6 DOF with $m = 185$ kg given by the following set of parameters:

$$\begin{aligned} \boldsymbol{M} &= \text{diag}\{215,\, 265,\, 265,\, 40,\, 80,\, 80\} \\ \boldsymbol{D}(\boldsymbol{\nu}) &= \text{diag}\{70,\, 100,\, 100,\, 30,\, 50,\, 50\} \\ &+ \text{diag}\{100|u|,\, 200|v|,\, 200|w|,\, 50|p|,\, 100|q|,\, 100|r|\} \end{aligned}$$

with $\boldsymbol{C}(\boldsymbol{\nu})$ given by (23). The vehicle is assumed to be neutrally buoyant. Environmental disturbances such as waves and currents were not incorporated in the simulation models. Hence integral action was not implemented. The control law parameters were chosen as $\boldsymbol{\Lambda} = \boldsymbol{K}_P = \boldsymbol{K}_D = \boldsymbol{I}$ and $\boldsymbol{K}_I = \boldsymbol{0}$ (with the appropriate dimensions). The desired position $\boldsymbol{x}_d$ was generated by a 2nd-order filter:

$$\ddot{\boldsymbol{x}}_d + 2\lambda_x \dot{\boldsymbol{x}}_d + \lambda_x^2 \boldsymbol{x}_d = \lambda_x^2 \boldsymbol{x}_r$$

where $\lambda_x = 0.75$ and $\boldsymbol{x}_r$ was chosen as a square wave between 0 and 5 (m) with period 20 (sec). The desired attitude signal was generated from an axis-angle parameterization of $SO(3)$, that is $\boldsymbol{R}_d = \boldsymbol{R}(\boldsymbol{n}_d, \alpha_d)$. The axis was chosen constant $\boldsymbol{n}_d = (1/\sqrt{3})\,[1,\, 1,\, -1]^{\mathrm{T}}$ whereas the desired angle α_d was generated by a 2nd-order filter:

$$\ddot{\alpha}_d + 2\lambda_\alpha \dot{\alpha}_d + \lambda_\alpha^2 \alpha_d = \lambda_\alpha^2 \alpha_r$$

where $\lambda_\alpha = 1$ and α_r was chosen as a square wave between 0 and $2\pi/3$ (rad) with period 20 (sec). The desired attitudes were computed according to:

1. Vector quaternion: $\quad \boldsymbol{\epsilon}_d = \sin\dfrac{\alpha_d}{2}\boldsymbol{n}_d$
2. Euler rotation: $\quad (\eta\boldsymbol{\epsilon})_d = \dfrac{1}{2}\sin\alpha_d \boldsymbol{n}_d$
3. Rodrigues parameters: $\quad (\boldsymbol{\epsilon}/\eta)_d = \tan\dfrac{\alpha_d}{2}\boldsymbol{n}_d$
4. Unit quaternion: $\quad \eta_d = \cos\dfrac{\alpha_d}{2}, \qquad \boldsymbol{\epsilon}_d = \sin\dfrac{\alpha_d}{2}\boldsymbol{n}_d$

The vectors $\dot{\boldsymbol{\xi}}_d$ and $\ddot{\boldsymbol{\xi}}_d$ were calculated from the kinematic equations utilizing:

$$\boldsymbol{\omega}_d = \dot{\alpha}_d\, \boldsymbol{n}_d \;\Rightarrow\; \dot{\boldsymbol{\omega}}_d = \ddot{\alpha}_d\, \boldsymbol{n}_d$$

The initial values were $\tilde{\boldsymbol{\xi}}(0) = \tilde{\boldsymbol{\xi}}_j(0) = \boldsymbol{0}$ and $\dot{\tilde{\boldsymbol{\xi}}}(0) = \dot{\tilde{\boldsymbol{\xi}}}_j(0) = \boldsymbol{0}$ $(j = 1...3)$. Runge-Kutta's 4th-order method with sampling time 0.1 (sec) was used in the simulations. Figure 1 shows

the simulation results for the control law in Section 3.1. Both the translational and the rotational tracking error is satisfactory, as we can see from the lower left and lower right plots.

For RPY representation of attitude, the reference trajectory at $\alpha_d = 2\pi/3$ corresponds to the singular configuration $\theta_d = \pi/2$, where θ_d is the desired pitch angle. The Euler angle model was simulated, but α_d was reduced in two different runs with a factor of 0.9825 and 0.9826, respectively. The reference Euler angles were found through the angle-axis representation of SO(3). Figure 2 shows the Euler angles ϕ, θ and ψ and the tracking errors for $\alpha_d := 0.9825\,\alpha_d$ in the left plots, and $\alpha_d := 0.9826\,\alpha_d$ in the right plots. Both the rotational and the translational tracking errors are satisfactory for pitch angles less than about 88.5°, but they are unstable for larger values. Similar results were obtained near the singularities of the 3-parameter representations of Section 3.

5 Conclusions

A 6 DOF attitude and position tracking controller has been derived by extending the results of [19]. Unit quaternion is used for attitude representation. Hence, singularities due to three parameters in the representation are avoided.

For completeness, it has also been shown how some alternative quaternion based 3-parameter representations of attitude can be applied in the control scheme. This extends the results of Slotine and Benedetto [18] and Fossen and Sagatun [9].

The simulation study indicates that the overall system performance is excellent in the unit quaternion feedback case. With 3-parameter attitude representations the tracking performance is excellent except in the vicinity of the representation singularities.

6 Acknowledgments

This work was supported by the Royal Norwegian Council for Scientific and Industrial Research through the MOBATEL Program at The Norwegian Institute of Technology, University of Trondheim.

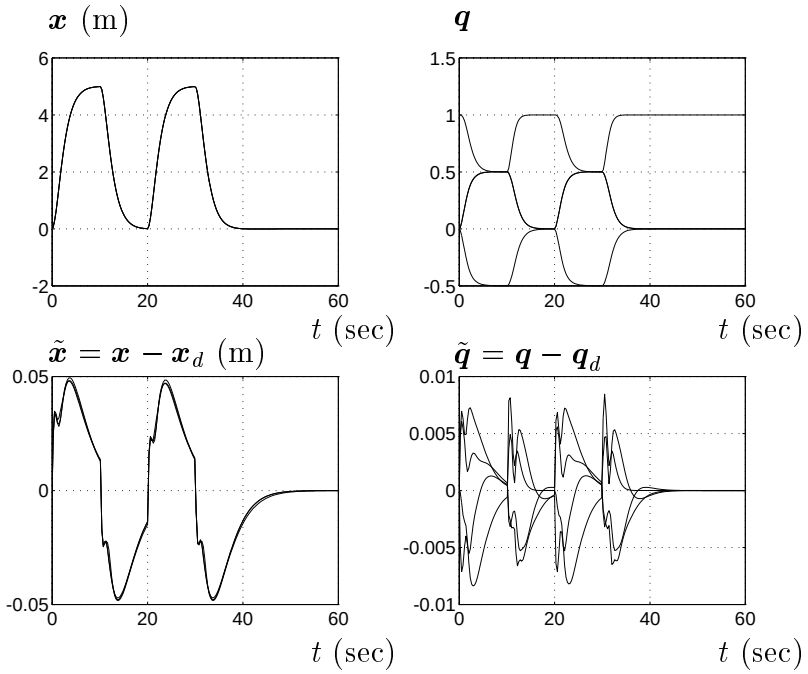

Figure 1: Tracking in terms of unit quaternion feedback using vector algebra attitude error. The position vector and the corresponding tracking errors are shown in the left plots, whereas the attitude and the attitude tracking errors are shown in the right plots.

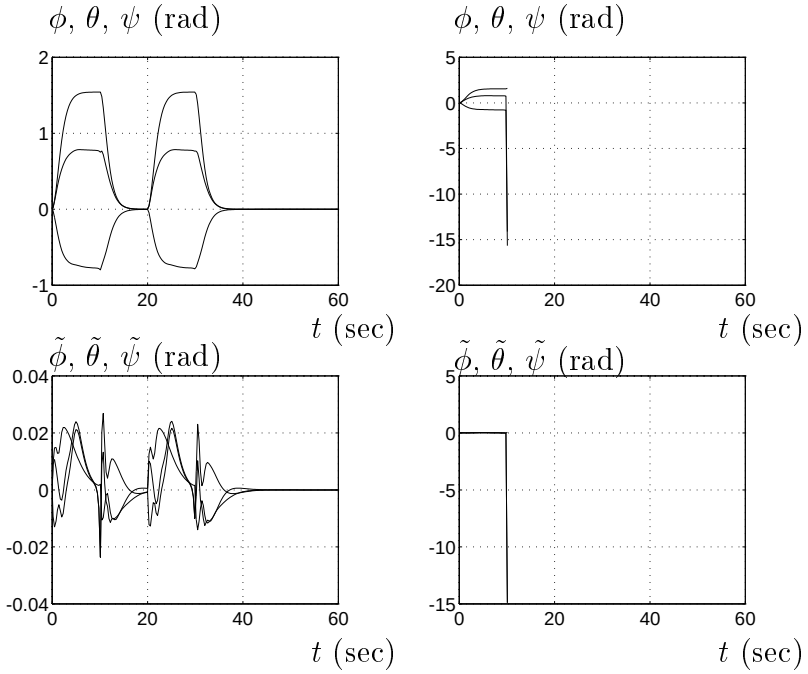

Figure 2: Tracking in terms of RPY Euler angle feedback. The attitude and the attitude tracking errors are shown in the left plots for $\alpha_d := 0.9825\,\alpha_d$, and in the right plots for $\alpha_d := 0.9826\,\alpha_d$ (unstable). The instability occurs when the pitch angle exceeds circa 88.5°.

References

[1] I. Barbălat. Systèmes d'Équations Différentielles d'Oscillations Non Linéaires. *Revue de Mathématiques Pures et Appliquées*, 4(2):267–270, 1959. Académie de la République Populaire Roumaine (in French).

[2] T. A. W. Dwyer, III. Exact Nonlinear Control of Large Angle Rotational Maneuvres. *IEEE Transactions on Automatic Control*, 29(9):769–774, 1984.

[3] O. Egeland and J.-M. Godhavn. Passivity Based Adaptive Attitude Control of a Rigid Spacecraft. *IEEE Transactions on Automatic Control*, 39(3), 1994.

[4] O. M. Faltinsen. *Sea Loads on Ships and Offshore Structures.* Cambridge University Press, 1990.

[5] O.-E. Fjellstad and T. I. Fossen. Comments on "The Attitude Control Problem". *IEEE Transactions on Automatic Control*, 39(3):699–700, 1994.

[6] O.-E. Fjellstad and T. I. Fossen. Quaternion Feedback Regulation of Underwater Vehicles. In *Proceedings of the 3rd IEEE Conference on Control Application*, Glasgow, Scotland, U.K., Aug. 24-26, 1994.

[7] T. I. Fossen. Comments on "Hamiltonian Adaptive Control of Spacecraft". *IEEE Transactions on Automatic Control*, 38(4):671–672, 1993.

[8] T. I. Fossen. *Guidance and Control of Ocean Vehicles.* John Wiley & Sons Ltd., 1994.

[9] T. I. Fossen and S. I. Sagatun. Adaptive Control of Nonlinear Underwater Robotic Systems. In *Proceedings of the 1991 IEEE Conference on Robotics and Automation*, pages 1687–1695, Sacramento, California, apr 1991.

[10] H. Goldstein. *Classical Mechanics.* Addison-Wesley, 1980.

[11] P. C. Hughes. *Spacecraft Attitude Dynamics.* John Wiley & Sons, 1986.

[12] F. H. Imlay. The Complete Expressions for Added Mass of a Rigid Body Moving in an Ideal Fluid. Technical Report DTMB 1528, David Taylor Model Basin, Washington D.C., 1961.

[13] H. K. Khalil. *Nonlinear Systems.* Macmillan, 1992.

[14] G. Kirchhoff. *Über die Bewegung eines Rotationskorpers in einer Flussigkeit.* Crelle's Journal, No. 71, pp. 237-273 (in German), 1869.

[15] G. Meyer. Design and Global Analysis of Spacecraft Attitude Control Systems. Technical Report NASA TR R-361, National Aeronautics and Space Administration, Washington D.C., 1971.

[16] R. E. Mortensen. A Globally Stable Linear Attitude Regulator. *International Journal of Control*, 8(3):297–302, 1968.

[17] S. V. Salehi and E. P. Ryans. A Non-Linear Feedback Attitude Regulator. *International Journal of Control*, 41(1):281–287, 1985.

[18] J. J. E. Slotine and M. D. Di Benedetto. Hamiltonian Adaptive Control of Spacecraft. *IEEE Transactions on Automatic Control*, 35(7):848–852, 1990.

[19] J. J. E. Slotine and W. Li. On the Adaptive Control of Robot Manipulators. *The International Journal of Robotics Research*, 6(3):49–59, 1987.

[20] J. Stuelpnagel. On the Parametrization of the Three-Dimensional Rotation Group. *SIAM Review*, 6(4):422–430, 1964.

[21] J. T. Y. Wen and K. Kreutz-Delgado. The Attitude Control Problem. *IEEE Transactions on Automatic Control*, 36(10):1148–1162, 1991.

[22] K. Wendel. Hydrodynamic Masses and Hydrodynamic Moment of Inertia. Technical report, TMB Translation 260, July 1956.

[23] B. Wie, H. Weiss, and A. Arapostathis. Quaternion Feedback Regulator for Spacecraft Eigenaxis Rotations. *AIAA Journal of Guidance, Control and Dynamics*, 12(3):375–380, 1989.

[24] R. G. J. Winchester. Astable ROV Design Concept Strutural Inspection Device Version (S.I.D.). *Underwater Technology*, 15(4):11, 1989.